

# Isolation and characterization of a motility-defective mutant of *Euglena gracilis*

Shuki Muramatsu<sup>1,2</sup>, Kohei Atsuji<sup>3,4</sup>, Koji Yamada<sup>Corresp., 3,4</sup>, Kazunari Ozasa<sup>4</sup>, Hideyuki Suzuki<sup>3</sup>, Takuto Takeuchi<sup>3</sup>, Yuka Hashimoto-Marukawa<sup>3,4</sup>, Yusuke Kazama<sup>4,5</sup>, Tomoko Abe<sup>4</sup>, Kengo Suzuki<sup>Corresp., 3,4</sup>, Osamu Iwata<sup>3</sup>

<sup>1</sup> Showa Women's University, Tokyo, Japan

<sup>2</sup> Euglena Co., Ltd., Tokyo, Japan

<sup>3</sup> euglena Co., Ltd., Tokyo, Japan

<sup>4</sup> RIKEN, Wako, Japan

<sup>5</sup> Fukui Prefectural University, Fukui, Japan

Corresponding Authors: Koji Yamada, Kengo Suzuki

Email address: yamada@euglena.jp, suzuki@euglena.jp

*Euglena gracilis* is a green photosynthetic microalga that swims using its flagellum. This species has been used as a model organism for over half a century to study its metabolism and the mechanisms of its behavior. The development of mass-cultivation technology has led to *E. gracilis* application as a feedstock in various products such as foods. Therefore, breeding of *E. gracilis* has been attempted to improve the productivity of this feedstock for potential industrial applications. For this purpose, a characteristic that preserves the microalgal energy e.g., reduces motility, should be added to the cultivars. The objective of this study was to verify our hypothesis that *E. gracilis* locomotion-defective mutants are suitable for industrial applications because they save the energy required for locomotion. To test this hypothesis, we screened for *E. gracilis* mutants from Fe-ion-irradiated cell suspensions and established a mutant strain, M<sub>3</sub>ZFeL, which shows defects in flagellum formation and locomotion. The mutant strain exhibits a growth rate comparable to that of the wild type when cultured under autotrophic conditions, but had a slightly slower growth under heterotrophic conditions. It also stores 1.6 times the amount of paramylon, a crystal of  $\beta$ -1,3-glucan, under autotrophic culture conditions, and shows a faster sedimentation compared with that of the wild type, because of the deficiency in mobility and probably the high amount of paramylon accumulation. Such characteristics make *E. gracilis* mutant cells suitable for cost-effective mass cultivation and harvesting.

1

## 2 **Isolation and characterization of a motility-defective** 3 **mutant of *Euglena gracilis***

4

5

6 Shuki Muramatsu <sup>1,†</sup>, Kohei Atsuji <sup>1,2</sup>, Koji Yamada <sup>1,2</sup>, Kazunari Ozasa <sup>3</sup>, Hideyuki Suzuki <sup>1</sup>,  
7 Takuto Takeuchi <sup>1</sup>, Yuka Hashimoto-Marukawa <sup>1,2</sup>, Yusuke Kazama <sup>4,‡</sup>, Tomoko Abe<sup>4</sup>, Kengo  
8 Suzuki<sup>1,2</sup>, Osamu Iwata<sup>1,2</sup>

9 <sup>1</sup> R&D Department, euglena Co., Ltd., Minatot-ku, Tokyo, Japan

10 <sup>2</sup> Microalgae Production Control Technology Laboratory, RIKEN, Wako, Saitama, Japan

11 <sup>3</sup> Bioengineering Laboratory, RIKEN, Wako, Saitama, Japan

12 <sup>4</sup> Nishina Center for Accelerator-based Science, RIKEN, Wako, Saitama, Japan

13

14

15 † Present affiliation:

16 Faculty of Life and Environmental Sciences, Showa Women's University, Setagauya-ku Tokyo,  
17 Japan

18

19 ‡ Present affiliation:

20 Department of Bioscience and Biotechnology, Fukui Prefectural University, Yoshida-gun, Fukui,  
21 Japan

22

23

24 Corresponding Author:

25 Koji Yamada <sup>1,2</sup>

26 5-29-11 Shiba, Minato-ku, Tokyo 108-0014, Japan

27 Email address: [yamada@euglena.jp](mailto:yamada@euglena.jp)

28

29 Kengo Suzuki<sup>1,2</sup>

30 5-29-11 Shiba, Minato-ku, Tokyo 108-0014, Japan

31 Email address: [suzuki@euglena.jp](mailto:suzuki@euglena.jp)

32

33 Osamu Iwata <sup>1,2</sup>

34 5-29-11 Shiba, Minato-ku, Tokyo 108-0014, Japan

35 Email address: [iwata@euglena.jp](mailto:iwata@euglena.jp)

36

37

**38 Abstract**

39 *Euglena gracilis* is a green photosynthetic microalga that swims using its flagellum. This species  
40 has been used as a model organism for over half a century to study its metabolism and the  
41 mechanisms of its behavior. The development of mass-cultivation technology has led to *E.*  
42 *gracilis* application as a feedstock in various products such as foods. Therefore, breeding of *E.*  
43 *gracilis* has been attempted to improve the productivity of this feedstock for potential industrial  
44 applications. For this purpose, a characteristic that preserves the microalgal energy e.g., reduces  
45 motility, should be added to the cultivars. The objective of this study was to verify our  
46 hypothesis that *E. gracilis* locomotion-defective mutants are suitable for industrial applications  
47 because they save the energy required for locomotion. To test this hypothesis, we screened for *E.*  
48 *gracilis* mutants from Fe-ion-irradiated cell suspensions and established a mutant strain, M<sup>-</sup>  
49 <sub>3ZFeL</sub>, which shows defects in flagellum formation and locomotion. The mutant strain exhibits a  
50 growth rate comparable to that of the wild type when cultured under autotrophic conditions, but  
51 had a slightly slower growth under heterotrophic conditions. It also stores 1.6 times the amount  
52 of paramylon, a crystal of β-1,3-glucan, under autotrophic culture conditions, and shows a faster  
53 sedimentation compared with that of the wild type, because of the deficiency in mobility and  
54 probably the high amount of paramylon accumulation. Such characteristics make *E. gracilis*  
55 mutant cells suitable for cost-effective mass cultivation and harvesting.

56

**57 Introduction**

58 The locomotion of organisms is directly linked to characteristic evolutionary survival  
59 competitions, such as acquiring food, finding suitable environments, and escaping from predators  
60 (Domenici et al. 2007). Locomotion in response to environmental stimuli is defined as “taxis,”  
61 including chemotaxis, gravitaxis, and phototaxis, which respectively refer to locomotion toward  
62 chemicals, gravity, and light, respectively (Dusenbery 2009). Such taxes are essential for  
63 organisms to survive in natural environments and are regulated by complex mechanisms (Webre  
64 et al. 2003; Okita 2005; Roberts 2006; Jékely et al. 2008; Roberts 2010; Sourjik and Wingreen  
65 2012). The means of locomotion depend on the organism size and are optimized through  
66 evolution (Jahn and Bovee 1965; Dusenbery 1997). Many of the motile unicellular  
67 microorganisms in the hydrosphere use their flagella to swim (Miyata et al. 2020).

68

69 Among the microalgae, *Chlamydomonas reinhardtii* has been widely used as a model  
70 organism to study the molecular mechanisms underlying the swimming of phytoplankton cells  
71 using their flagella. *C. reinhardtii* is used as a model microalga because its genetic methodology  
72 has been established (Harris 2001). Using their gravitaxis and phototaxis, strategies to screen  
73 non-motile *C. reinhardtii* mutants were developed (Kamiya 1991). The acquisition of these  
74 mutants and their analysis elucidated the molecular mechanisms used for swimming; e.g. the  
75 interaction between microtubule and dynein motor protein drives the motion of the flagella  
76 (Kamiya and Okamoto 1985; Kamiya et al. 1991; Kamiya 1995). The photosynthetic flagellate

77 species of the genus *Euglena* also use their flagella to swim, but they can be shed in response to  
78 chemical or mechanical stimuli (Bovee 1982). In contrast to *Chlamydomonas* cells, which cannot  
79 change their shape, *Euglena* spp. demonstrate an amoeboid movement called “euglenoid  
80 movement” without a flagellum, although it is an extremely slow means of migration (Bovee  
81 1982).

82

83 *Euglena gracilis* is extensively used as a model organism to study the mechanisms of  
84 photosynthesis, cell metabolism, and locomotive behaviors, such as gravitaxis and phototaxis  
85 (Richter et al. 2002; Daiker et al. 2010, 2011; Schwartzbach and Shigeoka 2017). Recent  
86 advances in experimental techniques, such as gene knockdown, have facilitated *E. gracilis* gene  
87 function studies. For example, a photoactivated adenylyl cyclase was reported to be required as a  
88 photoreceptor for phototaxis (Iseki et al. 2002). In contrast, it remains very difficult to obtain  
89 nuclear mutants of *E. gracilis*; few traits are induced by mutagens, such as ultraviolet light or  
90 ethyl methanesulfonate, which has hampered the complete inhibition of a specific gene  
91 functions, and is suggested to be related to the species’ polyploidy (Schiff and Epstein 1965; Hill  
92 et al. 1966). Accordingly, few locomotion-defective mutant strains have been identified and  
93 characterized (Schiff et al. 1980). Although a chloroplast mutant of *E. gracilis*, M<sup>-</sup><sub>2</sub>BUL, was  
94 previously reported to lack motility (Shneyour and Avron 1975), it has not been extensively  
95 examined; it is reported to lack photosynthesis activity and is not available in current culture  
96 collections, e.g., The Sammlung von Algenkulturen der Universität Göttingen (Culture  
97 Collection of Algae at Göttingen University [SAG], DEU), to which various *E. gracilis* wild-  
98 type strains are deposited.

99

100 In addition to its utilization as a model organism, *E. gracilis* has been exploited for  
101 industrial applications because of its fast proliferation, nutrient-rich features, and characteristic  
102 metabolism (Schwartzbach and Shigeoka 2017). As a saccharide reserve, *E. gracilis* stores  
103 paramylon, a crystalline form of β-(1,3)-D-glucan, which has various applications in the food  
104 industry (Watanabe et al. 2013; Russo et al. 2017). Thus, *E. gracilis* cells are particularly suitable  
105 as an ingredient in functional foods and supplements. Moreover, the stored paramylon is  
106 metabolized under hypoxic conditions into wax ester, which is suitable as a biofuel source (Inui  
107 et al. 1982, 1983). To enhance these industrial applications, *E. gracilis* has been bred to achieve  
108 thermostability and high oil production using Fe-ion irradiation as a mutagen (Yamada et al.  
109 2016a, b).

110

111 In the present study, we produced and characterized a non-motile mutant strain of *E.*  
112 *gracilis* (M<sup>-</sup><sub>3</sub>ZFeL). We hypothesized that the non-motile mutant strain has a higher paramylon  
113 production than the wild type, because it could save significant energy, which is mostly used for  
114 the swimming in the wild type (Hamilton et al. 1992; Tunçay et al. 2013). We used our  
115 previously established method, which uses Fe-ion beam irradiation as a mutagen agent, to  
116 produce non-motile mutants of *E. gracilis* (Yamada et al. 2016a, b). We screened for non-motile

117 cells from the Fe-ion beam-irradiated population and selected M<sub>3</sub>ZFeL for further studies. The  
118 proliferation rate, swimming and sedimentation speed, and paramylon and wax ester production  
119 of M<sub>3</sub>ZFeL were measured. Our results demonstrated that Fe-ion beam irradiation and the  
120 following screening method was an efficient strategy necessary to acquire non-motile *E. gracilis*  
121 mutant strains, as well as the potential of the produced M<sub>3</sub>ZFeL strain for industrial application.  
122

123

## 124 **Materials & Methods**

### 125 *Strains, culture, and media*

126 The wild-type Z strain, which is identical to *E. gracilis* SAG 1224-5/25, was provided by the  
127 culture collection of the Institute of Applied Microbiology (IAM), University of Tokyo, Tokyo,  
128 JPN. The M<sub>3</sub>ZFeL mutant strain produced in this study is deposited in the microbial culture  
129 collection at the National Institute for Environmental Studies (NIES, Tsukuba, JPN) with  
130 registration number NIES-4440. The cells were cultured using Cramer–Myers (CM) (Cramer and  
131 Myers 1952) and Koren–Hunter (KH) media (Koren and Hutner 1967) for autotrophic and  
132 heterotrophic growth, respectively, prepared at pH 3.5. The CM medium does not include a  
133 carbon source, while the KH medium includes 12 g L<sup>-1</sup> of glucose and various organic acids and  
134 amino acids as carbon sources. The seed culture was maintained in KH medium with each month  
135 of subculture.  
136

### 137 *Fe-ion irradiation and mutant screening*

138 The mutant strain was obtained through Fe-ion irradiation using the same conditions as  
139 previously reported (Yamada et al. 2016a, b), and mutant screening was based on the algal  
140 phenotypes. Two milliliters of an *E. gracilis* cell suspension (4 × 10<sup>5</sup> cells mL<sup>-1</sup>) was placed in  
141 hybridization bags that were segmented into 5 × 7 cm compartments. They were then irradiated  
142 by Fe ions (linear energy transfer [LET]: 650 keV μm<sup>-1</sup>) at a dose of 50 Gy in the RIKEN RI-  
143 beam factory (Wako, Saitama, JPN). After one week of recovery by culture inoculation in KH  
144 culture medium, two rounds of mutant screening were conducted.

145 About 1 × 10<sup>5</sup> mutagenized cells with independent genetic backgrounds were placed at  
146 one end of a culture dish filled with 10 mL of liquid KH medium with 0.5% methyl cellulose,  
147 which was added to solidify and prevent unexpected stirring of the culture, and were illuminated  
148 from the opposite end with 50 μmol photons m<sup>-2</sup> s<sup>-1</sup> of fluorescent light. After one week of  
149 culture incubation following Fe-ion beam irradiation, cells proliferated more than 100 times,  
150 resulting in 1 × 10<sup>7</sup> mutagenized cells, and most of them were found at the illuminated side  
151 through phototaxis. About 1,000 of the cells remained at the initial inoculation point; these were  
152 collected as putative non-motile mutant cells with a micropipette.

153 The collected population was supposed to include a high proportion of motile cells,  
154 which resided at the initial inoculation point due to random dispersal; therefore, they were  
155 subjected to a second round of screening. The cells were placed at the opening end of a 15 mL  
156 conical tube filled with 5 mL of liquid KH medium with 0.5% methyl cellulose, illuminated with

157 50  $\mu\text{mol photons m}^{-2} \text{ s}^{-1}$  of fluorescent light, and shaded with aluminum foil, except at the  
158 closing end. After 2 weeks of static horizontal incubation in the tubes, the cells proliferated more  
159 than 1,000 times. Most cells were gathered at the unshaded end to seek light. We retrieved about  
160 1,000 of the cells that showed no movement from the initial inoculation position and cultured  
161 them for an additional two weeks.

162 The proliferated cells were randomly isolated using fluorescence-activated cell sorting  
163 (MoFlo XDP; Beckman Coulter, Brea, CA, USA) to establish clonal lines in individual wells of  
164 96-well plates (Tissue Culture Test Plate; TPP, Trasadingen, CHE) filled with 200  $\mu\text{L}$  of KH  
165 medium. Populations without cell motility were selected by microscopic observations at 26 °C  
166 and identified as the motility-defective strains. The above-mentioned screening was performed  
167 for two independently mutagenized populations. During the screening process, cells proliferated  
168 more than  $10^6$  times; therefore, each population included many genetically identical cells. Based  
169 on this possibility, one mutant strain was established from each population, i.e., two strains were  
170 established from the two independent populations.

171

### 172 *Morphological characterization*

173 The cells were observed under an upright light microscope (DM2500B; Leica, Wetzlar, DEU)  
174 equipped with a differential interference contrast module. Scanning electron microscopy (SEM)  
175 was conducted using a field emission scanning electron microscope (SU8200; Hitachi, Tokyo,  
176 JPN) after following a general sample preparation. Briefly, 1 mL of culture in KH medium was  
177 centrifuged at  $2,000 \times g$  for 1 min to collect the cells. The precipitated cells were pre-fixed by  
178 adding a solution containing 2.5% glutaraldehyde, 2% paraformaldehyde, and 0.1 M sodium  
179 cacodylate, and fixed again using a solution containing 1% osmium tetroxide and 0.1 M sodium  
180 cacodylate. The fixed samples were completely dried using a critical point dryer, sputter-coated  
181 with osmium, and then subjected to SEM photographing.

182 For quantifying the proportion of cells with flagella, the cells were cultured in CM or  
183 KH medium and used in their logarithmic growth phase for analysis. For the CM medium, the  
184 cells were cultured in 50 mL of medium using a 100 mL volume test tube aerated with 50 mL  
185  $\text{min}^{-1}$  of air containing 5%  $\text{CO}_2$ . For the KH medium, each strain was cultured in 50 mL of  
186 medium using a 100 mL volume conical flask with rotary shaking at 100 rpm. Each culture was  
187 conducted at 26 °C with  $100 \mu\text{mol m}^{-2} \text{ s}^{-1}$  of constant illumination and sub-cultured every week  
188 to maintain a stable proliferation. The cells were then fixed with glutaraldehyde (0.025%) and  
189 observed for the presence of flagella under an inverted microscope (CKX41; Olympus, Tokyo,  
190 JPN) equipped with a phase contrast module. To exclude subjective judgment, short and intact  
191 flagella were not differentiated and were counted as cells with flagella.

192

### 193 *Growth tests*

194 The algae growth rate was evaluated in 100 mL test tubes containing 50 mL of medium. The  
195 cells were inoculated with an initial optical density (OD) of 0.1 and precultured for three days in  
196 100 mL volume conical flasks containing KH medium with continuous shaking (100 rpm at 26

197 °C, and  $100 \text{ m}^{-2} \text{ s}^{-1}$  of constant illumination). The cultured cells were then collected by  
198 centrifuging at  $2,000 \times g$  for 5 min and washed twice with either KH or CM medium, which was  
199 subsequently used for the culture test. Next, the cell suspension was inoculated in culture tubes  
200 with an initial OD of 0.1 and incubated at 26 °C with  $100 \text{ } \mu\text{mol m}^{-2} \text{ s}^{-1}$  of constant illumination.  
201 KH and CM cultures were aerated with  $50 \text{ mL min}^{-1}$  of air containing 5%  $\text{CO}_2$ . ODs from  
202 culture growth were determined over time by spectrophotometer (UVmini-1240; Shimadzu,  
203 Kyoto, JPN) at  $\lambda$  680 nm, immediately after placing the suspension in the cuvette.

204

#### 205 *Quantitative analysis of motility*

206 We used microscopic observations with video image capture to quantitatively evaluate algae  
207 motility. Observation and image processing techniques were used as previously reported (Ozasa  
208 et al. 2011). We confined the cells in suspension ( $0.7 \text{ } \mu\text{L}$ , containing 300–500 cells) in a closed  
209 circular polydimethylsiloxane (PDMS) micro-chamber (2.49 mm diameter and  $140 \text{ } \mu\text{m}$  depth),  
210 and observed red-light, bright-field transmission images with a  $5\times$  objective lens at 26 °C.  
211 Approximately 300–500 cells were measured in the micro-chamber. Cell movements were  
212 visualized by differentiating, thresholding, and superimposing the video images sequentially  
213 (trace image), and evaluated by counting the spatial sum of the trace pixels in the trace image  
214 (Ozasa et al. 2013, 2014). The number of trace pixels was named the “trace momentum” (TM)  
215 (Ozasa et al. 2013; Ozasa et al. 2014). The measurement rate of the TM values was 0.67 Hz (one  
216 frame per 1.6 s). The TM value is a fair measure of all locomotive activity observed within the  
217 chamber. The typical swimming traces were individually superimposed onto the cell distribution  
218 image and prepared as a binary image to demonstrate the cell’s swimming activity (Ozasa et al.  
219 2016).

220

#### 221 *Sedimentation analysis*

222 Cellular sedimentation rates in KH and CM media at 26 °C were evaluated in 1.5 mL  
223 microtubes. The culture was prepared as indicated above for the morphology analysis. In brief,  
224 when CM medium was used, cells were cultured in 100 mL volume test tubes with aeration,  
225 whereas with KH medium, they were cultured in a 100 mL volume conical flask with rotary  
226 shaking at 100 rpm. Each culture was conducted with constant light illumination ( $100 \text{ } \mu\text{mol m}^{-2}$   
227  $\text{s}^{-1}$ ). Culture ODs average at  $\lambda$  680 nm were 23.4 and 22.0 by KH culture, and 4.1 and 4.4 by  
228 CM culture of wild-type and  $\text{M}^{-3}\text{ZFeL}$  strains, respectively. Images of the cell suspension in  
229 each microtubule were taken at 1–5 min intervals with a general compact digital camera. The  
230 transparent supernatant area was detected and quantified from the images using the Image J  
231 software, with the threshold values set as 0 to 50 after converting to greyscale. Identical  
232 rectangular regions were selected inside the images of microtube images, and the transparent  
233 area inside each region was quantified.

234 To evaluate the sedimentation speed at 20 cm depth, the *E. gracilis* wild type and the  $\text{M}^{-}$   
235  $\text{3ZFeL}$  mutant strains were cultured in cuboid acryl beakers ( $10 \times 10 \times 30 \text{ cm}$ ) using 2 L of CM  
236 medium at 29 °C and  $1,300 \text{ } \mu\text{mol m}^{-2} \text{ s}^{-1}$  of overhead illumination (light–dark ratio of 12:12 h).

237 Beakers were filled with approximately the same concentrations ( $\text{g L}^{-1}$ ) of cells, 0.37 and 0.32 g  
238  $\text{L}^{-1}$  for the wild-type and M<sub>3</sub>ZFeL strains, respectively. After stirring the culture, sedimentation  
239 was periodically observed for 3.5 h, and supernatant was carefully removed to obtain a  
240 concentrated culture. Sediment concentration was then quantified by weighing the dried cells  
241 after filtration with a glass fiber filter (GA-55; ADVANTEC, Tokyo, JPN).

242

#### 243 *Quantification of carbohydrates and lipids*

244 The harvested algal cells were freeze-dried (FDV-1200; EYELA, Tokyo, JPN), and the  
245 deproteinized paramylon and lipid components were extracted as previously reported (Inui et al.  
246 1982; Suzuki et al. 2015). The dried cells (10 mg) were sonicated twice in 10 mL of acetone for  
247 90 s (UD-201; TOMY, Tokyo, JPN) with dial setting at 4 in 50 mL volume of plastic centrifuge  
248 tubes. The paramylon was subsequently separated from the residual components using  
249 centrifugation, boiled for 30 min in 10 mL of 1% sodium dodecyl sulfate aqueous solution, and  
250 washed twice with 10 mL of water. The extracted paramylon was then quantified using the  
251 phenol–sulfuric acid method (Montgomery 1957), which can quantify total carbohydrates.  
252 Similarly, neutral lipids were extracted from 100 mg of dried cells using n-hexane as a solvent;  
253 10 mL of n-hexane was added to the dried cells in 50 mL glass centrifuge tubes. The suspension  
254 was then homogenized for 90 s using a sonicator (UD-201; TOMY, Tokyo, JPN) with dial  
255 setting at 4, and then filtered with a piece of glass fiber filter paper (GF/C; Whatman, Little  
256 Chalfont, Buckinghamshire, UK), followed by an additional step of residue extraction. After  
257 evaporating the collected organic solvent dissolving lipids, the weight of the residue left in the  
258 flask was quantified as that of the extracted total neutral lipid.

259

#### 260 *Statistical analyses*

261 The results with error bars, except that of motility quantification, are represented as mean  $\pm$   
262 standard error from three independent experiments. The results of motility quantification are  
263 represented as mean  $\pm$  standard deviation (SD) for the whole measured time points. Statistical  
264 significance was analyzed using Student's *t*-test. For multiple comparisons, Bonferroni's  
265 corrections were applied.  $p < 0.05$  was considered significant.

266

## 267 **Results**

268

#### 269 *Characterization of M<sub>3</sub>ZFeL*

270 Through our screening for non-motile mutants of *E. gracilis*, we established two mutants with  
271 independent genetic backgrounds. The mutant strains were named M<sub>3</sub>ZFeL and M<sub>4</sub>ZFeL  
272 according to the typical nomenclature (Schiff et al. 1980), with the phenotypic designation “M”  
273 for motility and the mutagen designation “Fe” for Fe-ion irradiation (Yamada et al. 2016a). The  
274 strain M<sub>3</sub>ZFeL showed a stable behavioral phenotype, and was thus used in this study.

275

276 The *E. gracilis* M<sub>3</sub>ZFeL strain showed non-motile phenotype with few defects in  
277 proliferation. This phenotype was identified by the formation of colonies from single-cell  
278 inoculation in liquid culture. The M<sub>3</sub>ZFeL strain showed colony formation in liquid KH culture  
279 medium after a week, whereas wild-type cells were dispersed in the same culture medium (Fig.  
280 1A and B). As judged by both light and electron microscopy, the M<sub>3</sub>ZFeL cells were more  
281 rounded than were the wild-type cells. In addition, the M<sub>3</sub>ZFeL flagella were shorter than those  
282 of the wild type (Fig. 1C–F). Moreover, a significantly higher proportion of M<sub>3</sub>ZFeL cells  
283 lacked flagella both in the CM ( $p = 5.6 \times 10^{-5}$ ,  $t(4) = 15.1$ ) and KH ( $p = 0.04$ ,  $t(4) = 2.29$ )  
284 media (Fig. 1G and H).

285

286 The autotrophic and heterotrophic growth rates of the wild-type and M<sub>3</sub>ZFeL strains were  
287 evaluated using KH and CM culture media (Fig. 2). The mutant strain showed slightly slower  
288 and faster growth than did the wild type in the KH and CM culture, respectively. The M<sub>3</sub>ZFeL  
289 culture ODs at the third ( $p = 0.020$ ,  $t(4) = -5.81$ ) and fourth ( $p = 1.5 \times 10^{-4}$ ,  $t(4) = -20.48$ ) days  
290 of KH culture, which included high amounts of glucose, were significantly lower than those of  
291 the wild type (Fig. 2A). On the other hand, the ODs on the second ( $p = 0.020$ ,  $t(4) = -6.13$ ),  
292 fourth ( $p = 0.042$ ,  $t(4) = -4.98$ ), and eleventh ( $p = 0.036$ ,  $t(4) = -5.18$ ) days of CM culture were  
293 significantly higher than those of the wild type (Fig. 2B).

294

295 Our quantification of motility showed that the M<sub>3</sub>ZFeL TM values were less than one-  
296 thousandth that of the wild type. Following previous studies, cells cultured in a liquid KH  
297 medium were adequately stirred and subjected to TM measurements. Fig. 3A shows the cell  
298 distribution and swimming traces over approximately 8 s. The absence of swimming traces for  
299 the mutant strain revealed that cells could not move using their flagella. The total TM value  $\pm$  SD  
300 for the wild-type strain was  $11,161 \pm 269$  for 368 cells, whereas that for M<sub>3</sub>ZFeL was only  $9 \pm$   
301  $6$  for 467 cells, as shown in Fig. 3B. The TM value for the mutant strain cannot be distinguished  
302 from the measurement noise, indicating that the M<sub>3</sub>ZFeL strain was almost completely non-  
303 motile. Although some of the M<sub>3</sub>ZFeL cells possessed a short flagellum (Fig. 1C–H), our results  
304 indicated that the short flagellum did not function well.

305

### 306 *Potential of M<sub>3</sub>ZFeL for industrial application*

307 M<sub>3</sub>ZFeL demonstrated faster sedimentation than did the wild type in 1.5 mL microtubes. As  
308 shown in Fig. 4, the M<sub>3</sub>ZFeL cell sedimentation rate was higher than that of the wild-type cells  
309 under both heterotrophic (Fig. 4A) and autotrophic (Fig. 4B) growth conditions using KH and  
310 CM media, respectively. The values at the final time point (40 min) were significantly different  
311 under both heterotrophic ( $p = 0.010$ ,  $t(4) = -3.69$ ) and autotrophic ( $p = 0.011$ ,  $t(4) = -3.60$ )  
312 conditions (Fig. 4A and B).

313

314 By analyzing sedimentation in a larger-scale culture, M<sub>3</sub>ZFeL was found to be  
315 advantageous for industrial harvesting. To assess the effect of fast sedimentation on the harvest

316 of cells cultured using photosynthesis, wild-type and  $M^{-3}$ ZFeL strains were cultured using CM  
317 medium and their sedimentation rates were measured in 20 cm-deep beakers.  $M^{-3}$ ZFeL cells  
318 showed a significantly faster sedimentation rate than did the wild-type cells (Fig. 5). The  $M^{-3}$   
319 ZFeL cell density at the bottom of the beaker ( $34.1 \text{ g L}^{-1}$ ), was more than 10 times that of the  
320 wild type ( $3.0 \text{ g L}^{-1}$ ).

321

322 The paramylon storage in  $M^{-3}$ ZFeL cells was equal to or greater than that in the wild-type  
323 cells, whereas lipid accumulation in  $M^{-3}$ ZFeL cells was less than (autotrophic) or equal to  
324 (heterotrophic) that that in the wild-type cells. As shown in Fig. 6A and B,  $M^{-3}$ ZFeL cells  
325 produced a higher amount of paramylon (1.6 times;  $p = 0.033$ ,  $t(4) = -2.51$ ) than did the wild-  
326 type cells under autotrophic conditions, whereas there was no significant difference under  
327 heterotrophic conditions. In contrast, the  $M^{-3}$ ZFeL strain showed a lower lipid content than did  
328 the wild type, especially under autotrophic conditions ( $p = 0.034$ ,  $t(4) = -2.47$ ). (Fig. 6C and D).

329

## 330 Discussion

331 The non-motile and fast sedimentation phenotypes of the  $M^{-3}$ ZFeL mutant strain were  
332 considered to have strong correlations with the loss of negative gravitaxis. Wild-type *E. gracilis*  
333 exhibited positive and negative gravitaxis that depended on its environmental and cellular status  
334 (Stallwitz and Häder 1994; Lebert et al. 1999). Recent research has shown that wild-type *E.*  
335 *gracilis* uses mechano-sensing proteins and flagellar beating to stay at a preferential water depth  
336 (Häder and Hemmersbach 2017), rather than using buoyancy control. Since  $M^{-3}$ ZFeL cells were  
337 incapable of flagellar beating, they could not use negative gravitaxis to prevent sinking. In  
338 addition, the highly accumulated paramylon, which had a particle density of approximately 1.5 in  
339  $M^{-3}$ ZFeL cells, may also contribute to the increase in their specific gravity and sinking under  
340 autotrophic conditions. Our sedimentation tests showed that the faster sedimentation of the  $M^{-3}$   
341 ZFeL cells was achieved not only in small microtubes but also inside a deeper reservoir, thus  
342 being advantageous for industrial harvesting. Typically, cells in heterotrophic cultures sediment  
343 faster than those in autotrophic cultures, probably due to the higher carbohydrate accumulation.  
344 However, our results in microtubes showed that both strains sedimented faster in the autotrophic  
345 culture than in the heterotrophic culture. This seems to be due to the differences in cell density of  
346 the cultures; stacking highly concentrated cells at the bottom of the KH culture inhibited further  
347 sedimentation of the cells.

348

349 Flagellar motion is derived from the driving force of the doublet microtubules and dynein  
350 in the flagellum. Defects in the dynein, axonemal proteins, or related components result in a lack  
351 of flagellar movement (Turner 2006; Wang et al. 2014). We have not yet identified the  
352 component, or more specifically, the gene, responsible for the immobility of the  $M^{-3}$ ZFeL  
353 mutant strain. However, the lack of motility possibly reduces the cellular energy consumption  
354 and glycolysis. Such suppression is reported to result in enhanced starch accumulation in

355 *Chlamydomonas* (Hamilton et al. 1992; Tunçay et al. 2013), which may explain why greater  
356 paramylon storage was observed in the M<sub>3</sub>ZFeL cells.

357

358 The M<sub>3</sub>ZFeL strain showed slightly slower growth in the heterotrophic KH culture than  
359 did the wild type, suggesting that the function of glucose metabolism was slightly disturbed in  
360 the mutant. Meanwhile, the M<sub>3</sub>ZFeL strain showed faster growth in the autotrophic CM culture,  
361 which did not include carbon sources, suggesting that the mutant strain had an intact  
362 photosynthesis system and consumed the photosynthesized resources slower than the wild type.  
363 Moreover, the M<sub>3</sub>ZFeL had no defect in paramylon production, thus indicating that M<sub>3</sub>ZFeL  
364 may improve industrial paramylon production. Although a limited defect was observed in the  
365 accumulation of lipids, M<sub>3</sub>ZFeL would also be applicable to lipid production. The higher  
366 accumulation of paramylon in M<sub>3</sub>ZFeL may be partially due to the energy conservation by not  
367 swimming. However, since the proliferation speed of M<sub>3</sub>ZFeL was not drastically faster than the  
368 wild type, even in the autotrophic culture, the amount of energy conservation in M<sub>3</sub>ZFeL does  
369 not seem significant.

370

371 The M<sub>3</sub>ZFeL characterization results suggest that the mutant is defective in the  
372 components related to flagellum motion and/or formation that are not critical for survival and  
373 proliferation, at least under controlled laboratory conditions. The production of mutant strains by  
374 mutagenesis using high-LET irradiations, such as Ar-ion or Fe-ion irradiation, is advantageous  
375 because it causes a small number of large deletions in the genome with few side mutations  
376 (Hirano et al. 2015; Kazama et al. 2017). Although we could not identify the genetic cause of the  
377 phenotype in M<sub>3</sub>ZFeL, the process of breeding these strains ensures minimal side mutations.  
378 This will enable the immediate industrial use of the strain by reducing the possibility of showing  
379 unexpected and undesirable traits, which may not be observed in the laboratory but appear under  
380 harsh and unstable outdoor-culture conditions.

381

382 The M<sub>3</sub>ZFeL mutant of *E. gracilis* produced in this study is highly promising for the  
383 industrial production of food ingredients and chemical substances because it evidenced fast  
384 sedimentation, high paramylon storage, and a growth speed comparable to that of the wild type,  
385 at least under autotrophic conditions. In particular, the fast sedimentation of the mutant strain  
386 will save time and energy during the harvesting processes, which will contribute to the use of *E.*  
387 *gracilis* as a feedstock for biofuel by improving the balance between the energy invested to  
388 produce it and the energy output. In practical cultivation to produce paramylon and lipid under  
389 autotrophic conditions, processes to accumulate respective ingredients are added. In particular,  
390 cultured cells are subjected to nitrogen-restricted conditions to accumulate paramylon; the  
391 culture is then condensed and hypoxically conditioned to ferment the paramylon to wax ester  
392 (Suzuki 2017). Our results showed that M<sub>3</sub>ZFeL can competently accumulate larger amounts of  
393 paramylon under heterotrophic culture conditions than under autotrophic conditions; therefore,  
394 we suggest that they also show sufficient paramylon accumulation by nitrogen restriction (Briand

395 and Calvayrac 1980; Sumida et al. 1987), which enables the subsequent accumulation of wax  
396 ester (Inui et al. 2017). In contrast, the fast-sinking trait of the cells may cause sedimentation in  
397 industrial-scale culture ponds during cultivation. To test this and improve the mass-cultivation  
398 method, further experiments using practical outdoor-culture ponds are required.

399

400 In addition to the production cost, non-motile cells have the advantage of being easy to  
401 observe and manipulate in a limited area under the microscope. This will be helpful for further  
402 basic studies on *E. gracilis*, which should include a long-lasting evaluation of a specific cell, e.g.,  
403 observing its basic physiological phenomena, such as cell division (Figure S1 and Supplemental  
404 movie), as well as the micro-manipulation of single cells, such as that through single-cell  
405 electroporation, to deliver genes and proteins to the cells (Ohmachi et al. 2016).

406

407

## 408 **Conclusions**

409 This study demonstrated the successful production of a motility-defective mutant of the  
410 microalga *E. gracilis*, which has been industrially used in recent years. The acquired mutant  
411 showed amoebic motility but no swimming using the flagellum, and accumulated more  
412 carbohydrates than did the wild type under autotrophic culture conditions. However, the growth  
413 results indicated that the energy conservation due to the non-motile phenotype was not  
414 significant. Instead, owing to the inability to migrate and the accumulation of carbohydrates with  
415 high specific gravity, the cells sedimented faster during incubation. This trait indicates the  
416 potential to save energy for harvesting by introducing a natural sedimentation process. Therefore,  
417 the produced motility-defective mutant of *E. gracilis* and its derivatives may be useful for the  
418 industrial production of *E. gracilis*.

419

420

## 421 **Acknowledgments**

422 The heavy-ion beam irradiation was conducted at the RI beam factory (RIBF), which is operated  
423 by the RIKEN Nishina Center and Center for Nuclear Study, University of Tokyo. The SEM  
424 images of the cells were obtained with the assistance of Dr. Toyooka (RIKEN, CSRS, JPN). We  
425 would like to thank Editage ([www.editage.com](http://www.editage.com)) for English language editing.

426

427

## 428 **References**

- 429 Bovee EC (1982) Movement and locomotion of Euglena. In: The Biology of EUGLENA  
430 Volume III: Physiology. Academic Press, New York., pp 143–168  
431 Briand J, Calvayrac R (1980) Paramylon synthesis in heterotrophic and photoheterotrophic  
432 *Euglena* (euglenophyceae). J Phycol 16:234–239  
433 Cramer M, Myers J (1952) Growth and photosynthetic characteristics of *Euglena gracilis*.  
434 17:384–402

- 435 Daiker V, Häder D-P, Richter PR, Lebert M (2011) The involvement of a protein kinase in  
436 phototaxis and gravitaxis of *Euglena gracilis*. *Planta* 233:1055–1062. doi: 10.1007/s00425-  
437 011-1364-5
- 438 Daiker V, Lebert M, Richter P, Häder D-P (2010) Molecular characterization of a calmodulin  
439 involved in the signal transduction chain of gravitaxis in *Euglena gracilis*. *Planta* 231:1229–  
440 1236. doi: 10.1007/s00425-010-1126-9
- 441 Dusenbery, DB (2009) *Living at micro scale: the unexpected physics of being small*. Harvard  
442 University Press ( Cambridge, MA); ISBN: 978-0-674-03116-6.
- 443 Domenici P, Claireaux G, McKenzie DJ (2007) Environmental constraints upon locomotion and  
444 predator-prey interactions in aquatic organisms: an introduction. *Philos Trans R Soc Lond B*  
445 *Biol Sci* 362:1929–36 . doi: 10.1098/rstb.2007.2078
- 446 Dusenbery DB (1997) Minimum size limit for useful locomotion by free-swimming microbes.  
447 *Proc Natl Acad Sci U S A* 94:10949–54. doi: 10.1073/pnas.94.20.10949
- 448 Häder D-P, Hemmersbach R (2017) Gravitaxis in *Euglena*. *Adv Exp Med Biol* 979:237–266.  
449 doi: 10.1007/978-3-319-54910-1\_12
- 450 Hamilton BS, Nakamura K, Roncari DA (1992) Accumulation of starch in *Chlamydomonas*  
451 *reinhardtii* flagellar mutants. *Biochem Cell Biol* 70:255–8
- 452 Harris EH (2001) *Chlamydomonas* as a model organism. *Annu Rev Plant Physiol Plant Mol Biol*  
453 52:363–406. doi: 10.1146/annurev.arplant.52.1.363
- 454 Hill HZ, Schiff J, Epstein HT (1966) Studies of chloroplast development in *Euglena*. *Biophys J*  
455 6:373–383. doi: 10.1038/185825a0
- 456 Hirano T, Kazama Y, Ishii K, Ohbu S, Shirakawa Y, Abe T (2015) Comprehensive identification  
457 of mutations induced by heavy-ion beam irradiation in *Arabidopsis thaliana*. *Plant J* 82:93–  
458 104. doi: 10.1111/tpj.12793
- 459 Inui H, Ishikawa T, Tamoi M (2017) Wax Ester Fermentation and Its Application for Biofuel  
460 Production. *Adv Exp Med Biol* 979:269–283. doi: 10.1007/978-3-319-54910-1\_13
- 461 Inui H, Miyatake K, Nakano Y, Kitaoka S (1983) Production and composition of wax esters by  
462 fermentation of *Euglena gracilis*. *Agric Biol Chem* 47:2669–2671. doi:  
463 10.1080/00021369.1983.10866013
- 464 Inui H, Miyatake K, Nakano Y, Kitaoka S (1982) Wax ester fermentation in *Euglena gracilis*.  
465 *FEBS Lett* 150:89–93. doi: 10.1016/0014-5793(82)81310-0
- 466 Iseki M, Matsunaga S, Murakami A, Ohno K, Shiga K, Yoshida K, Sugai M, Takahashi T, Hori  
467 T, Watanabe M (2002) A blue-light-activated adenylyl cyclase mediates photoavoidance in  
468 *Euglena gracilis*. *Nature* 415:1047–1051. doi: 10.1038/4151047a
- 469 Jahn TL, Bovee EC (1965) Movement and locomotion of microorganisms. *Annu Rev Microbiol*  
470 19:21–58. doi: 10.1146/annurev.mi.19.100165.000321
- 471 Jékely G, Colombelli J, Hausen H, Guy K, Stelzer E, Nédélec F, Arendt D (2008) Mechanism of  
472 phototaxis in marine zooplankton. *Nature* 456:395–399. doi: 10.1038/nature07590
- 473 Kamiya R (1991) Selection of *Chlamydomonas* dynein mutants. *Methods Enzymol* 196:348–55.  
474 doi: 10.1016/0076-6879(91)96031-1
- 475 Kamiya R (1995) Exploring the function of inner and outer dynein arms with *Chlamydomonas*  
476 mutants. *Cell Motil Cytoskeleton* 32:98–102. doi: 10.1002/cm.970320205

- 477 Kamiya R, Kurimoto E, Muto E (1991) Two types of *Chlamydomonas* flagellar mutants missing  
478 different components of inner-arm dynein. *J Cell Biol* 112:441–7. doi:  
479 10.1083/jcb.112.3.441
- 480 Kamiya R, Okamoto M (1985) A mutant of *Chlamydomonas reinhardtii* that lacks the flagellar  
481 outer dynein arm but can swim. *J Cell Sci* 74:181–91
- 482 Kazama Y, Ishii K, Hirano T, Wakana T, Yamada M, Ohbu S, Abe T (2017) Different  
483 mutational function of low- and high-linear energy transfer heavy-ion irradiation  
484 demonstrated by whole-genome resequencing of *Arabidopsis* mutants. *Plant J* 92:1020–  
485 1030. doi: 10.1111/tbj.13738
- 486 Koren LE, Hutner SH (1967) High-yield media for photosynthesizing *Euglena gracilis* Z. *J*  
487 *Protozool* 14:(Suppl.) 17
- 488 Miyata M, Robinson RC, Uyeda TQP, Fukumori Y, Fukushima S-I, Haruta S, Homma M, Inaba  
489 K, Ito M, Kaito C, Kato K, Kenri T, Kinoshita Y, Kojima S, Minamino T, Mori H, Nakamura  
490 S, Nakane D, Nakayama K, Nishiyama M, Shibata S, Shimabukuro K, Tamakoshi M,  
491 Taoka A, Tashiro Y, Tulum I, Wada H, Wakabayashi K-I (2020) Tree of motility - A  
492 proposed history of motility systems in the tree of life. *Genes Cells* 25:6–21. doi:  
493 10.1111/gtc.12737
- 494 Lebert M, Porst M, Richter P, Hader DP (1999) Physical characterization of gravitaxis in  
495 *Euglena gracilis*. *J Plant Physiol* 155:338–43. doi: 10.1016/s0176-1617(99)80114-x
- 496 Montgomery R (1957) Determination of glycogen. *Arch Biochem Biophys* 67:378–386. doi:  
497 10.1016/0003-9861(57)90292-8
- 498 Ohmachi M, Fujiwara Y, Muramatsu S, Yamada K, Iwata O, Suzuki K, Wang DO (2016) A  
499 modified single-cell electroporation method for molecule delivery into a motile protist,  
500 *Euglena gracilis*. *J Microbiol Methods* 130:106–111. doi: 10.1016/j.mimet.2016.08.018
- 501 Okita N (2005) Phototactic activity in *Chlamydomonas* “non-phototactic” mutants deficient in  
502 Ca<sup>2+</sup>-dependent control of flagellar dominance or in inner-arm dynein. *J Cell Sci* 118:529–  
503 537. doi: 10.1242/jcs.01633
- 504 Ozasa K, Lee J, Song S, Hara M, Maeda M (2011) Two-dimensional optical feedback control of  
505 *Euglena* confined in closed-type microfluidic channels. *Lab Chip* 11:1933. doi:  
506 10.1039/c0lc00719f
- 507 Ozasa K, Lee J, Song S, Hara M, Maeda M (2013) Gas/liquid sensing via chemotaxis of *Euglena*  
508 cells confined in an isolated micro-aquarium. *Lab Chip* 13:4033. doi: 10.1039/c3lc50696g
- 509 Ozasa K, Lee J, Song S, Maeda M (2014) Transient freezing behavior in photophobic responses  
510 of *Euglena gracilis* investigated in a microfluidic device. *Plant Cell Physiol* 55:1704–1712.  
511 doi: 10.1093/pcp/pcu101
- 512 Ozasa K, Won J, Song S, Maeda M (2016) Autonomous oscillation/separation of cell density  
513 artificially induced by optical interlink feedback as designed interaction between two  
514 isolated microalgae chips. *Sci Rep* 6:24602. doi: 10.1038/srep24602
- 515 Richter P, Ntefidou M, Streb C, Lebert M, Hader D-P (2002) Physiological characterization of  
516 gravitaxis in *Euglena gracilis*. *J Gravit Physiol* 9: 279-280
- 517 Roberts AM (2010) The mechanics of gravitaxis in *Paramecium*. *J Exp Biol* 213:4158–4162.  
518 doi: 10.1242/jeb.050666

- 519 Roberts AM (2006) Mechanisms of gravitaxis in *Chlamydomonas*. Biol Bull 210:78–80. doi:  
520 10.2307/4134597
- 521 Russo R, Barsanti L, Evangelista V, Frassanito AM, Longo V, Pucci L, Penno G, Gualtieri P  
522 (2017) *Euglena gracilis* paramylon activates human lymphocytes by upregulating pro-  
523 inflammatory factors. Food Sci Nutr 5:205–214. doi: 10.1002/fsn3.383
- 524 Schiff JA, Epstein HT (1965) The continuity of the chloroplast in *Euglena*. In: Locke M (ed)  
525 Reproduction: Molecular, subcellular, and cellular. Academic Press, New York, pp 131–  
526 189
- 527 Schiff JA, Lyman H, Russell GK (1980) [2] Isolation of mutants of *Euglena gracilis*: An  
528 addendum. Methods Enzymol 69:23–29. doi: 10.1016/S0076-6879(80)69004-1
- 529 Schwartzbach SD, Shigeoka S (eds) (2017) *Euglena*: Biochemistry, cell and molecular biology.  
530 Springer International Publishing, Cham
- 531 Shneyour A, Avron M (1975) Properties of photosynthetic mutants isolated from *Euglena*  
532 *gracilis*. Plant Physiol 55:137–141
- 533 Sourjik V, Wingreen NS (2012) Responding to chemical gradients: bacterial chemotaxis. Curr  
534 Opin Cell Biol 24:262–268. doi: 10.1016/j.ceb.2011.11.008
- 535 Stallwitz E, Hader DP (1994) Effects of heavy metals on motility and gravitactic orientation of  
536 the flagellate, *Euglena gracilis*. Eur J Protistol 30:18–24. doi: 10.1016/s0932-  
537 4739(11)80194-x
- 538 Sumida S, Ehara T, Osafune T, Hase E (1987) Ammonia- and light-induced degradation of  
539 paramylum in *Euglena gracilis*. Plant Cell Physiol 28:1587–1592
- 540 Suzuki K (2017) Large-Scale Cultivation of *Euglena*. Adv Exp Med Biol 979:285–293. doi:  
541 10.1007/978-3-319-54910-1\_14
- 542 Suzuki K, Mitra S, Iwata O, Ishikawa T, Kato S, Yamada K (2015) Selection and  
543 characterization of *Euglena anabaena* var. *minor* as a new candidate *Euglena* species for  
544 industrial application. Biosci Biotechnol Biochem 79:.. doi:  
545 10.1080/09168451.2015.1045828
- 546 Tunçay H, Findinier J, Duchêne T, Coge V, Cousin C, Peltier G, Ball SG, Dauvillée D (2013) A  
547 forward genetic approach in *Chlamydomonas reinhardtii* as a strategy for exploring starch  
548 catabolism. PLoS One 8:e74763. doi: 10.1371/journal.pone.0074763
- 549 Turner RM (2006) Moving to the beat: a review of mammalian sperm motility regulation.  
550 Reprod Fertil Dev 18:25. doi: 10.1071/RD05120
- 551 Wang H, Gau B, Slade WO, Juergens M, Li P, Hicks LM (2014) The Global Phosphoproteome  
552 of *Chlamydomonas reinhardtii* reveals complex organellar phosphorylation in the flagella  
553 and thylakoid membrane. Mol Cell Proteomics 13:2337–2353. doi:  
554 10.1074/mcp.M114.038281
- 555 Watanabe T, Shimada R, Matsuyama A, Yuasa M, Sawamura H, Yoshida E, Suzuki K (2013)  
556 Antitumor activity of the  $\beta$ -glucan paramylon from *Euglena* against preneoplastic colonic  
557 aberrant crypt foci in mice. Food Funct 4:1685–1690. doi: 10.1039/c3fo60256g
- 558 Webre DJ, Wolanin PM, Stock JB (2003) Bacterial chemotaxis. Curr Biol 13:R47-9

559 Yamada K, Kazama Y, Mitra S, Marukawa Y, Arashida R, Abe T, Ishikawa T, Suzuki K (2016a)  
560 Production of a thermal stress resistant mutant *Euglena gracilis* strain using Fe-ion beam  
561 irradiation. Biosci Biotechnol Biochem 8451:1–7. doi: 10.1080/09168451.2016.1171702  
562 Yamada K, Suzuki H, Takeuchi T, Kazama Y, Mitra S, Abe T, Goda K, Suzuki K, Iwata O  
563 (2016b) Efficient selective breeding of live oil-rich *Euglena gracilis* with fluorescence-  
564 activated cell sorting. Sci Rep 6:26327. doi: 10.1038/srep26327  
565  
566

# Figure 1

Fig. 1.  $M_3ZFeL$  and wild-type strains of *Euglena gracilis* in static culture

(A and B) Photographs of wild-type (A) and  $M_3ZFeL$  (B) colonies grown in Koren-Hunter (KH) medium on a 96-well plate for one week. (C-F) Microphotographs (C and D) and scanning electron micrographs (E and F) of wild-type (C and E) and  $M_3ZFeL$  (D and F) cells cultured in 100 mL volume conical flasks containing KH medium with continuous shaking (100 rpm, 26 °C, and  $100 \mu\text{mol m}^{-2} \text{s}^{-1}$  of constant illumination). Scale bars indicate 20  $\mu\text{m}$ . (G and H) The proportion of cells that possess flagella among the wild-type and  $M_3ZFeL$  cells in the Cramer-Myers (CM) (G) and KH media (H). More than 200 cells were observed for each condition in one day. The observations were conducted three times on different days. Error bars show the standard errors for three replicates. \*  $p < 0.05$ , Student's  $t$ -test.

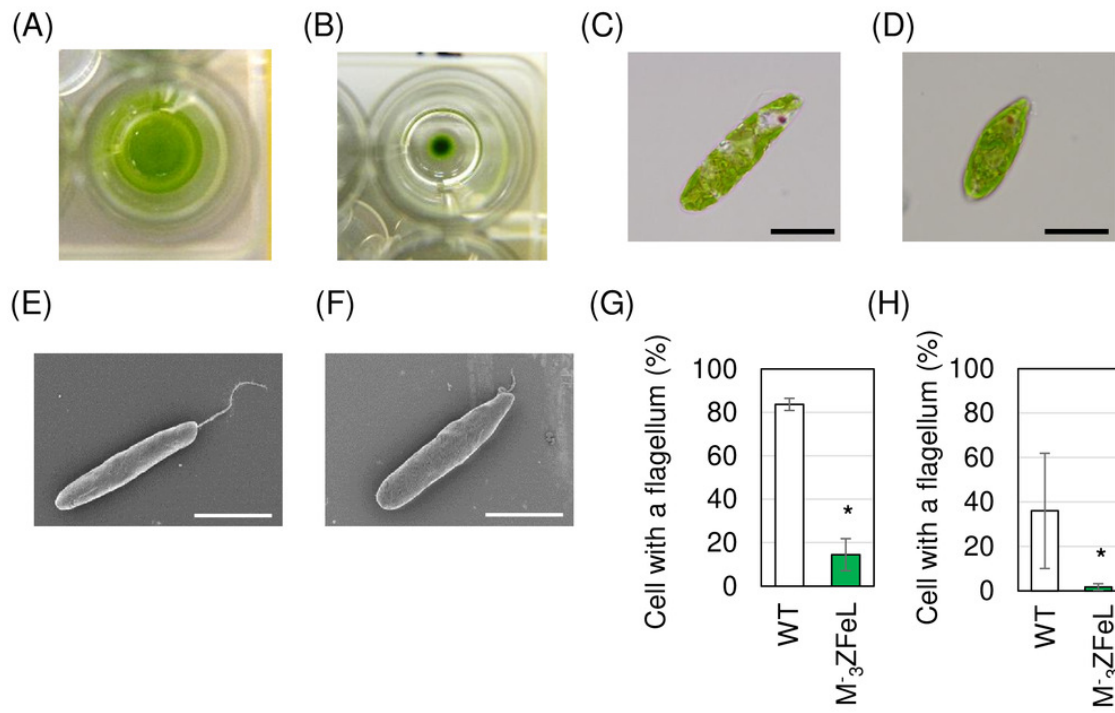


## Figure 2

Fig. 2. Growth curves of  $M_3ZFeL$  and wild-type strains of *Euglena gracilis*

(A and B) Growth curves of the wild-type (white) and  $M_3ZFeL$  (green) strains on heterotrophic KH (A) and autotrophic CM (B) media. The initial culture was inoculated into a medium with an optical density of 0.1 measured at  $\lambda$  680 nm. The growth was determined on days 0, 1, 2, 3, 4, 6, 7, 8, and 9 after the start of the Koren-Hunter (KH) culture, while it was determined on days 0, 1, 2, 4, 5, 7, 8, 10, 11, 14, and 15 after the start of the Cramer-Myers (CM) culture. The growth test was conducted in triplicate using three independent tubes. The error bars indicate the standard errors for these triplicates.  $*p < 0.05$ , Student's *t*-test with Bonferroni's correction.

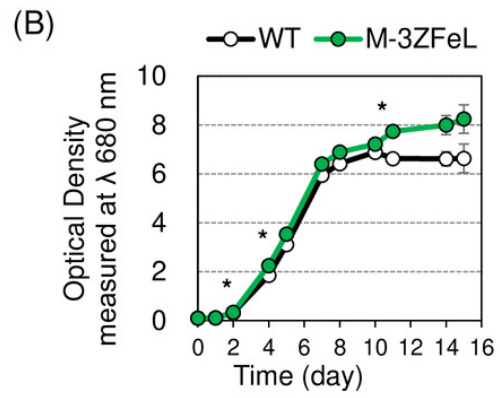
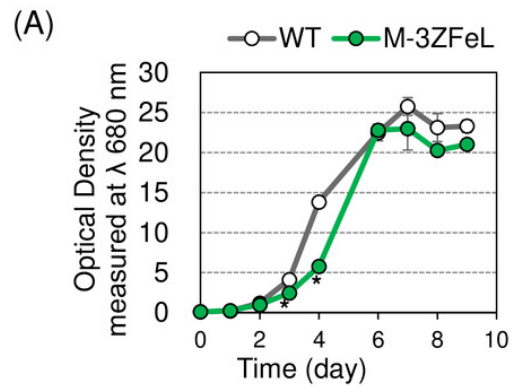


## Figure 3

Fig. 3. Motility quantification of  $M_3ZFeL$  and wild-type strains of *Euglena gracilis* using trace momentum (TM)

(A) Cell distribution and swimming traces over approximately 8 s for the wild-type (left panel) and  $M_3ZFeL$  (right panel) strains. Both cell types were grown in heterotrophic (KH) medium and measured during the logarithmic growth phase. The magnified images of the areas within the squares are shown in the lower left of the panels. The diameter of these circles are approximately 2.5 mm. Green dots and light green lines indicate *E. gracilis* cells and their traces, respectively. (B) The motility of the wild-type and  $M_3ZFeL$  strains, evaluated using TM. The TM was obtained every 1.6 s and averaged over 10 min. Error bars show the standard deviation for 500 time points.

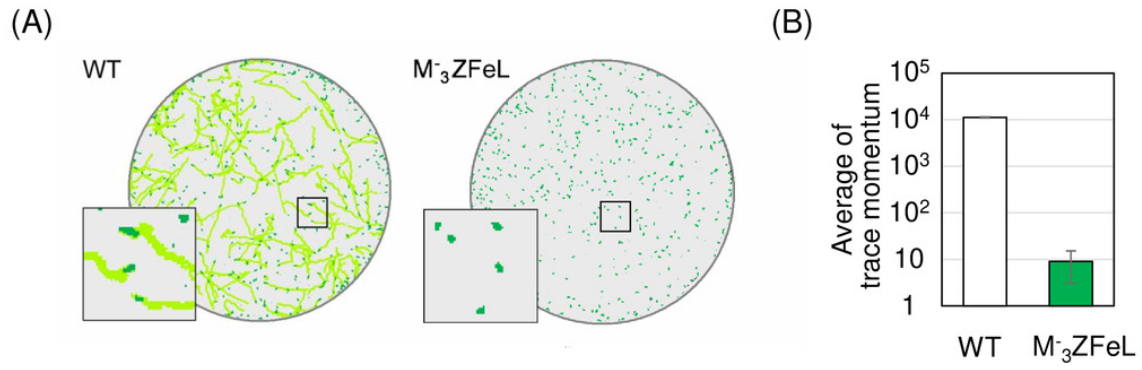


## Figure 4

Fig. 4. Sedimentation speed of M<sub>3</sub>ZFeL and wild-type strains of *Euglena gracilis*

(A and B) Sedimentation rates of the wild type (white) and M<sub>3</sub>ZFeL (green) in Koren-Hunter (KH) (heterotrophic; A) and Cramer-Myers (CM) (autotrophic; B) media. Photographs of the cell suspension were taken every 1 min to measure the transparent area in each 1.5 mL tube. After cell sedimentation, the supernatant becomes transparent, and the area on the photograph was used to evaluate the sedimentation rate. Error bars show standard errors for three replicates. a.u., arbitrary unit.

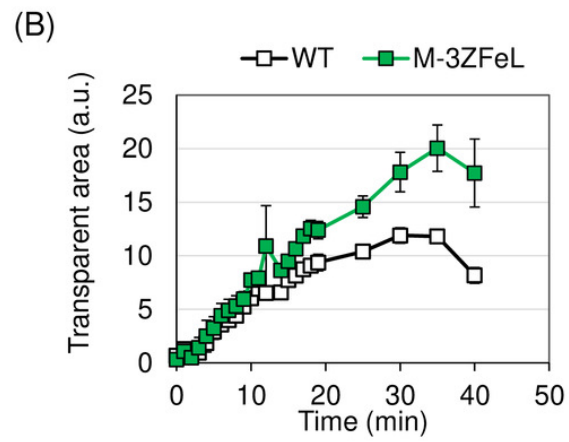
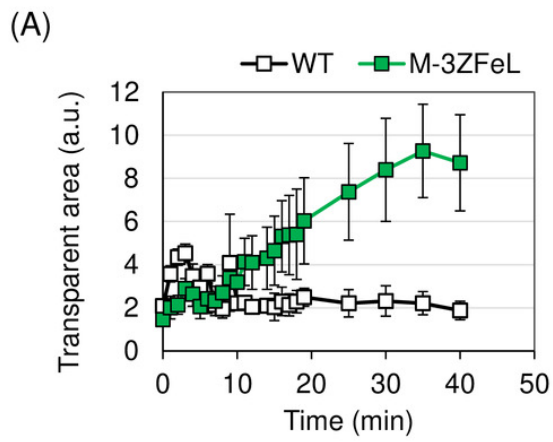
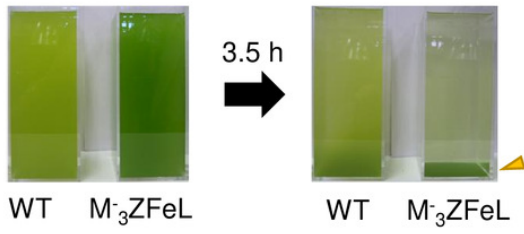


## Figure 5

Fig. 5. Sedimentation rate of *Euglena gracilis* cells in 20 cm-deep beakers

(A) Autotrophic cultures of the wild-type (left) and  $M_3ZFeL$  (right) strains suspended in 2 L beakers and left to stand under static conditions for 3.5 h. Cramer-Myers (CM) medium was used for the culture. (B) The sediment before and after 3.5 h of sedimentation. The cells that were retrieved from the bottom of the beaker and quantified for their dry weight are indicated with an arrowhead in (A).

(A)



(B)

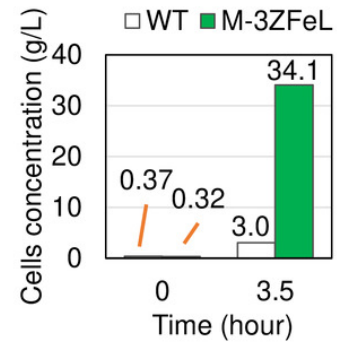


## Figure 6

Fig. 6. Paramylon storage and lipid content of M<sub>3</sub>ZFeL and wild-type strains of *Euglena gracilis* cells

(A-D) Paramylon storage (A and B) and lipid content (C and D) in the wild-type (white) and M<sub>3</sub>ZFeL (green) strains cultured in heterotrophic (A and C) and autotrophic (B and D) media. Paramylon and lipid were extracted and quantified from freeze-dried cells, and their percentage weights were calculated. Cells were collected during their logarithmic growth phase. The y-axis scale is different in each figure. Error bars show standard errors for three replicates. \* $p < 0.05$ , Student's *t*-test.

